

Conformationally Constrained 1,3-Diamino Ketones: A Series of Potent Inhibitors of the Cysteine Protease Cathepsin K

Robert W. Marquis,[†] Dennis S. Yamashita,[†] Yu Ru,[†] Stephen M. LoCastro,[†] Hye-Ja Oh,[†] Karl F. Erhard,[†] Renee L. DesJarlais,[‡] Martha S. Head,[‡] Ward W. Smith,[§] Baoguang Zhao,[§] Cheryl A. Janson,[§] Sherin S. Abdel-Meguid,[§] Thaddeus A. Tomaszek,^{||} Mark A. Levy,^{||} and Daniel F. Veber^{*,†}

Departments of Medicinal Chemistry, Structural and Physical Chemistry, Structural Biology, and Molecular Recognition, SmithKline Beecham Pharmaceuticals, 709 Swedeland Road, King of Prussia, Pennsylvania 19406

Received May 11, 1998

The maintenance of bone homeostasis is a dynamic equilibrium of bone formation by osteoblasts and resorption of the bone matrix by osteoclasts.¹ Shifts in this equilibrium toward the excessive resorption of bone matrix produce clinical manifestations such as osteoporosis, Paget's disease, and certain types of arthritis. Over the past several years cysteine proteases have been suggested to play a role in the osteoclast-mediated resorption of the bone matrix.² Recently it has been shown that cathepsin K (EC 3.4.22.38), a cysteine protease of the papain superfamily, is both selectively and highly expressed in osteoclasts.³ The implication of this abundant and selective expression suggests that this enzyme may be playing an important and specific role in the resorption phase of bone remodeling. Inhibition of this enzyme may therefore be a potential strategy for therapeutic intervention in diseases of excess bone resorption. Further support for this hypothesis is that mutations in the gene which encodes for this enzyme are associated with a rare autosomal disorder of bone remodeling known as pycnodysostosis.⁴ Also, Yamamura and co-workers have shown that a cathepsin K antisense construct inhibits osteoclastic bone resorption in pit formation.⁵

A series of potent, reversible inhibitors of cathepsin K based on a 1,3-bis(Cbz-Leu-amino)-2-propanone template has recently been disclosed from these laboratories.⁶ The design of these inhibitors was based on the observation that two aldehyde inhibitors, leupeptin (Ac-Leu-Leu-Arg-H) and Cbz-Leu-Leu-Leu-H, bound in opposite directions in the active site of papain. In an effort to design more potent inhibitors of cathepsin K, we have attempted to further exploit this design element by incorporating the 1,3-bis(Cbz-Leu-amino)-2-propanone inhibitor template **1** into conformationally constrained ring systems (see Figure 1). Historically, the introduction of a conformational constraint has been used to capture a bioactive orientation of a molecule.⁷

Modeling experiments based on the crystal structure of inhibitor **1** bound to the active site cysteine of

cathepsin K revealed that the enzyme could potentially accommodate cyclization of the 1,3-diamino ketone template in two alternative fashions with no deleterious steric interactions with the peptide backbone residues.⁸ As seen in Figure 1, cyclization of **1** along path A would produce the 2,5-diaminocyclopentanone and 2,6-diaminocyclohexanone inhibitors **2** and **3**. No overall reorganization of the original 1,3-diamino ketone template is observed in these analogues. Alternatively, cyclization along path B would provide the 3-aminopyrrolidinone and 4-aminopiperidinone inhibitors **4** and **5**, respectively. Molecular modeling revealed that this cyclization produces a change in the conformation of the original 1,3-diamino ketone substructure. All four of the proposed conformationally constrained scaffolds **2–5** have been modeled as tetrahedral adducts with the active site cysteine 25 of cathepsin K. The interactions between the inhibitor and enzyme have been optimized by overlapping the tetrahedral adducts with that from the inhibitor **1**/cathepsin K crystal structure, adjusting torsion angles to mimic the conformation of **1** bound to the enzyme. No apparent deleterious enzyme/inhibitor interactions were seen. Prediction of the binding of inhibitors using path B is much less obvious than for path A. Indeed, the exceptional differences in potency achieved by the analogues of path B compared to those of path A were not predicted and remain a matter of conjecture despite the extensive structure data available.

The designed inhibitors were synthesized as outlined in Scheme 1. Compounds **3** and **2** were synthesized via bis-acylation of the known racemic *trans*-1,3-diamino-2-cyclohexanol (**7**)¹² and by analogy the *trans*-1,3-diamino-2-cyclopentanol (**6**) with Cbz-leucine and HBTU to give the alcohols **9** and **8**. Jones oxidation gave the desired ketones **3** and **2**. The diastereomers of **2** were not separable and were therefore tested as a mixture. The diastereomeric mixture **3** was separable by silica gel chromatography, and each diastereomer was characterized as 1,3-*trans* by measuring the proton coupling constants ($J_{1ax,2ax} = 6.8$ Hz and $J_{1ax,2eq} = 3.3$ Hz) of the corresponding ketone-derived alcohols (NaBH₄/CH₃OH). On the basis of circular dichroism studies (n to π^* transitions of the cyclohexanones¹³), the absolute stereochemistries were assigned as *R,R* for the first eluted diastereomer and *S,S* for the second eluted diastereomer. Compounds **4** and **5** were synthesized as diastereomeric mixtures by EDC-mediated acylation of the amino alcohols **10**¹⁴ and **11**¹⁵ with Cbz-leucine. Deprotection of the Boc protecting group followed by a second EDC-mediated acylation gave the diastereomeric alcohols **12** and **13**. Oxidation of the alcohols was accomplished by employing either Jones reagent or Swern oxidation to give ketones **4** and **5**. The bis-Cbz-leucine-4-aminopyrrolidinone diastereomers **4** were separated by reverse-phase HPLC under neutral conditions (CH₃CN/pH = 7 phosphate buffer). These diastereomers were not configurationally stable and equilibrated to the original mixture upon concentration of the eluent. HPLC separation of the diastereomers of **5** revealed the

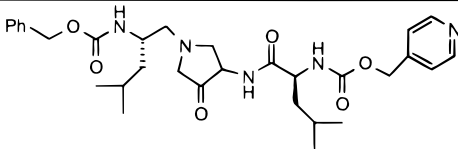
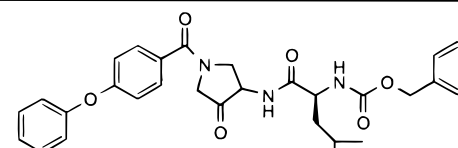
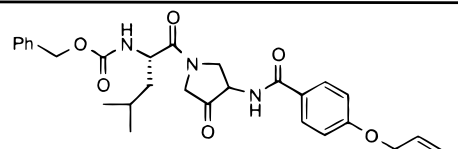
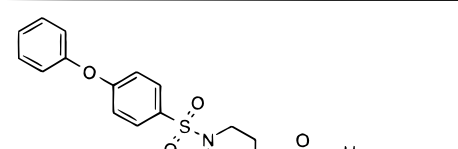
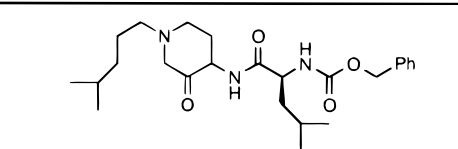
[†] Department of Medicinal Chemistry.

[‡] Department of Structural and Physical Chemistry.

[§] Department of Structural Biology.

^{||} Department of Molecular Recognition.

Table 1. Cathepsin K, B, and L Inhibition Data

Compound	Cat K $K_{i, app}$ (nM)	Cat B $K_{i, app}$ (nM)	Cat L $K_{i, app}$ (nM)
2	56 $M^{-1}s^{-1}$	-	-
3 (R,R)	16,000	-	-
3 (S,S)	15,000	-	-
4	2.3	>1000	39
5	2.6	440	16
12	3500	>1,000	>1,000
13	8200	>1,000	>1,000
	3.5	>1,000	120
	30	>1,000	55
	900	>1,000	>1,000
	0.5	>1,000	>1,000
	25	>1,000	>1,000

as it is consistent with a covalent interaction of the active site cysteine 25 with the carbonyl group of **4** to form a tetrahedral adduct (Figure 2). The hemith-

ioketal was flanked by the N1 Cbz-leucine which was observed to bind on the unprimed side of the active site.¹⁸ The isobutyl group of the leucine was bound in

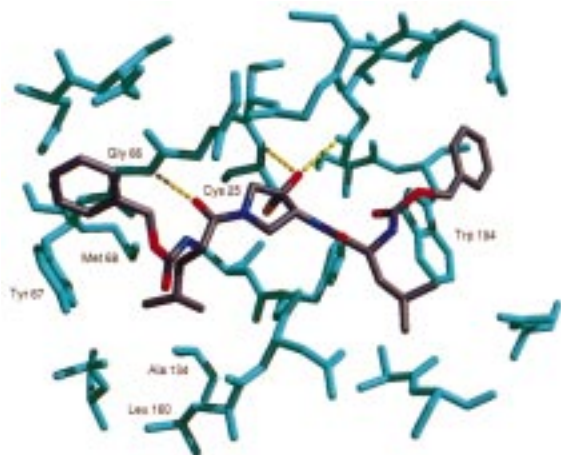


Figure 2. View of the X-ray cocrystal structure of inhibitor **4** bound in the active site of cathepsin K. The isobutyl group of the N1 Cbz-leucine lies buried in the hydrophobic S2 pocket formed by the side chains of Leu 160, Ala 134, and Met 68. A hydrogen bond is formed between the N1 amide carbonyl and Gly 66 of the enzyme.

the hydrophobic S2 pocket which was formed from the side-chain atoms of Leu 160, Ala 134, and Met 68. A hydrogen bond between the amide carbonyl of the N1 Cbz-leucine and Gly 66 of the protein backbone is also seen in the X-ray structure of **4** complexed with the enzyme. The N3 Cbz-leucine was seen bound on the primed side of the active site. The stereochemistry of the diastereomeric C3 center was consistent with the *R* configuration in the X-ray crystal structure and may therefore represent the more potent of the two diastereomeric forms. Alternatively, this stereochemical preference may be a function of crystal packing forces.

A possible rationalization for the dramatic difference in activities for the compounds resulting from the two different modes of cyclization is that, despite favorable modeling predictions and the presence of the correct specificity elements required for initial Michaelis binding in both sets of compounds, inhibitors **4** and **5** have the appended N1 amine group oriented in such a fashion as to allow for the facile attack by the active site cysteine nucleophile on the electrophilic carbonyl of the designed inhibitors. This may not be true for inhibitors **2** and **3** in which the diamino ketone template of **1** has essentially been substituted in both the α and α' positions. This substitution may cause a steric interaction which was unforeseen in the original modeling experiments on the thiol adducts.

As seen in Table 1, analogue **14** in which a methylene group has replaced the tertiary amide carbonyl moiety retains the overall potency of the parent cyclic diamino ketone **4**. The X-ray cocrystal structure of inhibitor **14** with cathepsin K shows no hydrogen bond in this region of the inhibitor/protein complex (see Figure 3). This change to a reduced amide has served to remove the amide linkage and simultaneously increase overall aqueous solubility. The leucine binding on the unprimed side of the active site of the enzyme could be replaced with several peptidomimetics and still retain the overall potency of this class. Analogue **15**, which incorporates a *p*-phenoxybenzamide peptidomimetic, results in a 13-fold loss of activity relative to **4**. Compound **16**, in which the leucine binding on the primed side of the active site

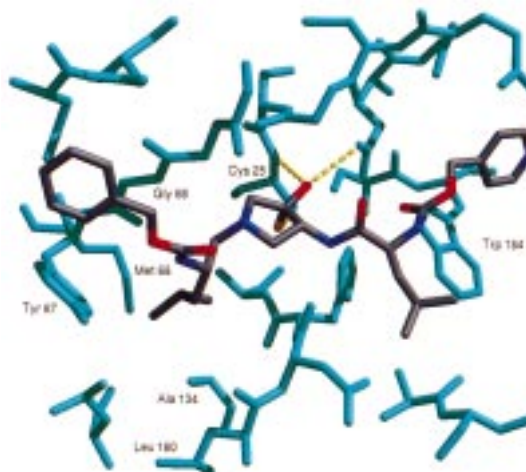


Figure 3. View of the X-ray cocrystal of inhibitor **14** bound in the active site of cathepsin K. The hydrogen bond between the N1 amide carbonyl of the inhibitor and Gly 66 of the enzyme that was present for inhibitor **4** is lacking in this inhibitor/enzyme complex.

has been replaced with the same *p*-phenoxybenzamide, is 30-fold less active relative to analogue **15**. Incorporation of the sulfonamide into the peptidomimetic gives the potent 4-phenoxybenzenesulfonamide derivative **17**. This modification has removed most of the structural liabilities commonly associated with peptide amide linkages. Complete removal of the peptide elements of the Cbz-leucine via the incorporation of a reduced amide while retaining the recognition element of the isohexyl group gave rise to analogue **18** which incorporates the *N*-isohexyl peptidomimetic.

In this communication we have disclosed a potent class of conformationally constrained ketone inhibitors of the cysteine protease cathepsin K. Peptidomimetic elements have been incorporated onto this scaffold which remove hydrogen bonding, a feature postulated to reduce rates of intestinal transfer.¹⁹ More detailed *in vivo* evaluation of such inhibitors will be the subject of future studies. The inhibition of other proteases may be possible with this cyclic diamino ketone template by the incorporation of the appropriate specificity elements required by these enzymes.

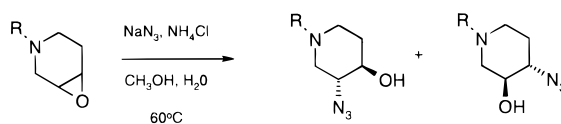
Acknowledgment. Dr. John Gleason and Dr. Brian Metcalf are thanked for their support of this work.

Supporting Information Available: Coordinates for compounds **4** and **14** bound to cathepsin K have been deposited in the Brookhaven Protein Databank, accession numbers 1AU3 and 1AU4, respectively. Crystallization data of cathepsin K complexed with **4** and **14** (2 pages). Ordering information is given on any current masthead page.

References

- (1) Baron, R. *Anatomy and Ultrastructure of Bone*. In *Primer on the Metabolic Bone Diseases and Disorders of Mineral Metabolism*, 1st ed.; Favus, M. J., Ed.; American Society for Bone and Mineral Research: Kelseyville, CA, 1990; pp 3–9.
- (2) (a) Votta, B. J.; Levy, M. A.; Badger, A.; Bradbeer, J.; Dodds, R. A.; James, I. A.; Thompson, S. T.; Bossard, M. J.; Carr, T.; Connor, J. R.; Tomaszek, T. A.; Szewczuk, L.; Drake, F. H.; Veber, D. F.; Gowen, M. Peptide Aldehyde Inhibitors of Cathepsin K Inhibit Bone Resorption Both *In Vitro* and *In Vivo*. *J. Bone Miner. Res.* **1997**, *12*, 1396–1406. (b) Delaisse, J.-M.; Eekhout, Y.; Vaes, G. *In Vivo* and *In Vitro* Evidence for the Involvement of Cysteine Proteinases in Bone Resorption. *Biochem. Biophys. Res. Commun.* **1984**, *125*, 441–447. (c) Delaisse,

- J. M.; Boyde, A.; Macconachie, E.; Ali, N. N.; Sear, C. H. J.; Eeckhout, Y.; Vaes, G.; Jones, S. J. The Effects of Inhibitors of Cysteine-Proteinases and Collagenase on the Resorptive Activity of Isolated Osteoclasts. *Bone* **1987**, *8*, 305–313.
- (3) (a) Drake, F. H.; Dodds, R. A.; James, I. A.; Connor, J. R.; Debouck, C.; Richardson, S.; Lee-Ryckaczewski, L.; Coleman, L.; Riemann, D.; Barthlow, R.; Hastings, G.; Gowen, M. Cathepsin K, but Not Cathepsin B, L or S is Abundantly Expressed in Human Osteoclasts. *J. Biol. Chem.* **1996**, *271*, 12511–12516. (b) Bromme, D.; Okamoto, K. Human Cathepsin O2, a Novel Cysteine Protease Highly Expressed in Osteoclastomas and Ovary. Molecular Cloning, Sequencing and Tissue Distribution. *Biol. Chem. Hoppe-Seyler* **1995**, *376*, 379–384. (c) Shi, G.-P.; Chapman, H. A.; Bhairi, S. M.; DeLeeuw, C.; Reddy, V. Y.; Weiss, S. J. Molecular Cloning of Human Cathepsin O, a Novel Endoproteinase and Homologue of Rabbit OC2. *FEBS Lett.* **1995**, *357*, 129–134. (d) Littlewood-Evans, A.; Kokubo, T.; Ishibashi, O.; Inaoka, T.; Wlodarski, B.; Gallagher, J. A.; Bilbe, G. Localization of Cathepsin K in Human Osteoclasts by *In Situ* Hybridization and Immunohistochemistry. *Bone* **1997**, *20*, 81–86. (e) Bossard, M. J.; Tomaszek, T. A.; Thompson, S. K.; Amegadzie, B. Y.; Hanning, C. R.; Jones, C.; Kurdyla, J. T.; McNulty, D. E.; Drake, F. H.; Gowen, M.; Levy, M. A. Proteolytic Activity of Human Osteoclast Cathepsin K. Expression, Activation, and Substrate Identification. *J. Biol. Chem.* **1996**, *271*, 12517–12524.
- (4) (a) Gelb, B. D.; Moissoglu, K.; Zhang, J.; Martignetti, J. A.; Bromme, D.; Desnick, R. J. Cathepsin K; Isolation and Characterization of the Murine cDNA and Genomic Sequence, the Homologue of the Human Pycnodysostosis Gene. *Biochem. Mol. Med.* **1996**, *59*, 200–206. (b) Johnson, M. R.; Polymeropoulos, M. H.; Vos, H. L.; Ortiz de Luna, R. I.; Francomano, C. A. A Nonsense Mutation in the Cathepsin K Gene Observed in a Family with Pycnodysostosis. *Genome Res.* **1996**, *6*, 1050–1055. (c) Gelb, B. D.; Shi, G.-P.; Chapman, H. A.; Desnick, R. J. Pycnodysostosis, A Lysosomal Disease Caused by Cathepsin K Deficiency. *Science* **1996**, *273*, 1236–1238.
- (5) Inui, T.; Ishibashi, O.; Inaoka, T.; Origane, Y.; Kumegawa, M.; Kokubo, T.; Yamamura, T. Cathepsin K Antisense Oligodeoxynucleotide Inhibits Osteoclastic Bone Resorption. *J. Biol. Chem.* **1997**, *272*, 8109–8112.
- (6) Yamashita, D. S.; Smith, W. W.; Zhao, B.; Janson, C. A.; Tomaszek, T. A.; Bossard, M. A.; Levy, M. A.; Oh, H.-J.; Carr, T. J.; Thompson, S. T.; Ijames, C. F.; Carr, S. A.; McQueney, M.; D'Alessio, K. J.; Amegadzie, B. Y.; Hanning, C. R.; Abdel-Meguid, S.; DesJarlais, R. L.; Gleason, J. G.; Veber, D. F. Structure and Design of Potent and Selective Cathepsin K Inhibitors. *J. Am. Chem. Soc.* **1997**, *119*, 11351–11352.
- (7) (a) Liskamp, R. M. J. Conformationally Restricted Amino Acids and Dipeptides, (Non)peptidomimetics and Secondary Structure Mimetics. *Recl. Trav. Chim. Pays-Bas* **1994**, *113*, 1–19. (b) Marshall, G. R.; Fedric, G. A.; Moore, M. L. Peptide Conformation and Biological Activity. *Annu. Rep. Med. Chem.* **1978**, *13*, 227–238.
- (8) The analogues were modeled with MacroModel version 5.5.⁹ The structures were then minimized using the MacroModel implementation of the AMBER¹⁰ force field and fit using UCSF MidasPlus.¹¹
- (9) Mohamadi, F.; Richards, N. G. J.; Guida, W. C.; Liskamp, R.; Lipton, M.; Caufield, C.; Chang, G.; Hendrickson, T.; Still, W. C. MacroModel-An Integrated Software System for Modeling Organic and Bioorganic Molecules Using Molecular Mechanics. *J. Comput. Chem.* **1990**, *11*, 440.
- (10) (a) Weiner, S. J.; Kollman, P. A.; Case, D. A.; Singh, U. C.; Ghio, C.; Alagona, G.; Profeta, S., Jr.; Weiner, P. A New Force Field for Molecular Mechanical Simulation of Nucleic Acids and Proteins. *J. Am. Chem. Soc.* **1984**, *106*, 765–784. (b) Weiner, S. J.; Kollman, P. A.; Nguyen, D. T.; Case, D. A. An All Atom Force Field for Simulations of Proteins and Nucleic Acids. *J. Comput. Chem.* **1986**, *7*, 230–252. (c) McDonald, D. Q.; Still, W. C. AMBER Torsional Parameters for the Peptide Backbone. *Tetrahedron Lett.* **1992**, *33*, 7743–7746.
- (11) Ferrin, T. E.; Huang, C. C.; Jarvis, L. E.; Langridge, R. The MIDAS Display System. *J. Mol. Graph.* **1988**, *6*, 13–27.
- (12) Sammes, P. G.; Thetford, D. Stereocontrolled Preparation of Cyclohexane Amino Alcohols Utilising a Modified Mitsunobu Reaction. *J. Chem. Soc. PTT* **1989**, 655–661.
- (13) Lightner, D. A.; Bouman, T. D.; Crist, B. V.; Rodgers, S. L.; Knobloch, M. A.; Jones, A. M. The Octant Rule. 21. Circular Dichroism Dependence on α -Methyl Configuration in Cyclohexanones. Experiments and RPA Calculations. *J. Am. Chem. Soc.* **1987**, *109*, 6248–6259 and references therein.
- (14) Hall, S. E.; Ballas, L. M.; Kulanthaivel, P.; Boros, C.; Jiang, J. B.; Jagdmann, G. E.; Lai, Y.-S.; Biggers, C. K.; Hu, H.; Hallock, Y.; Hughes, P. F.; DeFauw, J. M.; Lynch, M. P.; Lampe, J. W. C.; Menaldino, D. S.; Heerding, J. M.; Janzen, W. P.; Hollinshead, S. P. Balanoids. PCT Application WO 94/20062, 1994.
- (15) The Boc-protected amino alcohol **11** was prepared in an analogous fashion as that described for the Cbz derivative **27**. Treatment of epoxide **19** with sodium azide gave an inseparable mixture of azides **21** and **23** in a ratio of approximately 1:4–5 as determined by ¹H NMR analysis. The mixture of azido alcohols **21** and **23** was reduced by catalytic hydrogenation over 10% Pd/C in methanol to give the amino alcohols **25** and **11**. The undesired regioisomeric amino alcohol **25** was removed by column chromatography at a later stage in the synthesis. See: Lai, Y.-S.; Mendalino, D. S.; Nichols, J. B.; Jagdmann, G. E., Jr.; Mylott, F.; Gillespie, J.; Hall, S. E. Ring Size Effect in the PKC Inhibitory Activities of Perhydroazepine Analogues of Balanol. *Bioorg. Med. Chem. Lett.* **1995**, *5*, 2151–2154. In this paper the major product of sodium azide treatment of epoxide **20** is reported to be regioisomer **22** (4.8:1 **22**:**24**). In contrast to these results we have found that the desired regioisomer **24** is indeed the major product (4–5:1 **24**:**22**) of epoxide opening by sodium azide. These results have been confirmed by a series of ¹H NMR COSY studies on both **22** and **24**. This result was consistent with epoxide ring openings that have been reported for the analogous 3,4-epoxytetrahydropyrans. See: Berti, G.; Catelani, G.; Ferretti, M.; Monti, L. Regio- and Stereoselectivity of the three-membered Ring Opening of 3,4-Epoxytetrahydropyrans and of the Corresponding Epibromonium Ions. *Tetrahedron* **1974**, *30*, 4013–4020.



19 R = Boc

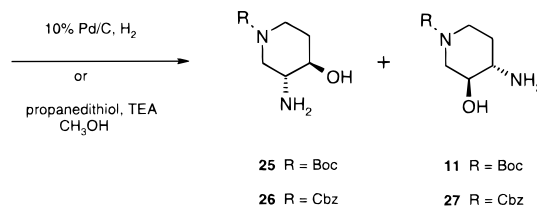
21 R = Boc

23 R = Boc

20 R = Cbz

22 R = Cbz

24 R = Cbz



25 R = Boc

11 R = Boc

26 R = Cbz

27 R = Cbz

- (16) Testing of the inhibitors was conducted with purified recombinant cathepsin K as described in ref 3e.
- (17) (a) Abeles, R. H. Enzyme Inhibitors: Ground State/Transition State Analogues. *Drug Dev. Res.* **1987**, *10*, 221–234. (b) Douglas, D. T. Transition-state Analogues in Drug Design. *Chem. Ind. (London)* **1983**, *8*, 311–315. (c) Brodbeck, U. Recent Developments in the Field of Enzyme Inhibitors. *Chimia* **1980**, *34*, 415–421. (d) Lienhard, G. E. Transition State Analogues as Enzyme Inhibitors. *Annu. Rep. Med. Chem.* **1972**, *7*, 249–258. (e) Radzika, A.; Wolfenden, R. Transition State and Multisubstrate Analogue Inhibitors. *Methods Enzymol.* **1995**, *249*, 284–312.
- (18) Schechter, I.; Berger, A. On the Size of the Active Site in Proteases. I. Papain. *Biochem. Biophys. Res. Commun.* **1967**, *27*, 157–162.
- (19) Spatola, A. Peptide Backbone Modifications: A Structure–Activity Analysis of Peptides Containing Amide Bond Surrogates, Conformational Constraints, and Related Backbone Replacements. *Chem. Biochem. Amino Acids Pept. Proteins* **1983**, *7*, 267–357.

JM980295F